

# Microwave dielectric properties of Ba(Sn<sub>x</sub>Zn<sub>(1-x)/3</sub>Nb<sub>(1-x)2/3</sub>)O<sub>3</sub> (0 ≤ x ≤ 0.32) ceramics

JWO-SHIUN SUN

*Department of Electronic Engineering, National Taipei Institute of Technology, Taipei, Taiwan*

JON-JER YU, JENG-CHEI YOU, CHUNG-CHUANG WEI

*Department of Electrical Engineering, National Cheng Kung University, Tainan, Taiwan*

The dielectric properties of the (1-x)Ba(Zn<sub>1/3</sub>Nb<sub>2/3</sub>)O<sub>3</sub>-xBaSnO<sub>3</sub> (0 ≤ x ≤ 0.32) composition at microwave frequencies were investigated in this study. With the addition of BaSnO<sub>3</sub>, the dielectric  $Q(Q_d)$  value of Ba(Zn<sub>1/3</sub>Nb<sub>2/3</sub>)O<sub>3</sub> (BZN) can be improved and a small temperature coefficient of resonant frequency ( $\tau_f$ ) can be achieved. When 22.6 mol % of Sn is added to BZN, the characteristics of the Ba(Sn<sub>0.226</sub>Zn<sub>0.258</sub>Nb<sub>0.516</sub>)O<sub>3</sub> ceramics sintered at 1500 °C are as follows: dielectric constant  $\epsilon_r = 32$ ,  $\tau_f = +12$  p.p.m. °C<sup>-1</sup> and high  $Q_d$  value of 9700 at 10 GHz. Based on the classical dispersion theory and the logarithmic mixing rule, the effects with additions of substitutional element of BaSnO<sub>3</sub> on the microwave dielectric properties of Ba(Zn<sub>1/3</sub>Nb<sub>2/3</sub>)O<sub>3</sub> can be mostly explained.

## 1. Introduction

A dielectric material acting as a resonator was first proposed by Richtmyer in 1939 [1]. With recent improvements, dielectric resonators (DRs) [2] with the small  $\tau_f$ , low loss and high  $\epsilon_r$  are widely used as the frequency-determining elements in microwave integrated circuits (MICs) such as dielectric resonator oscillators (DROs) [3], dielectric resonator filters (DRFs) [4], etc.

In recent years complex perovskite-type compounds with the chemical formula A<sup>2+</sup>(B<sub>1/3</sub><sup>2+</sup>B<sub>2/3</sub><sup>5+</sup>)O<sub>3</sub> have attracted considerable interest for use as high- $Q$  microwave dielectric resonators. These include Ba(Mg<sub>1/3</sub>Ta<sub>2/3</sub>)O<sub>3</sub> (BMT) [5], Ba(Zn<sub>1/3</sub>Ta<sub>2/3</sub>)O<sub>3</sub> (BZT) [6, 7], Ba(Zn<sub>1/3</sub>Nb<sub>2/3</sub>)O<sub>3</sub> (BZN) [8, 9], Ba(Ni<sub>1/3</sub>Nb<sub>2/3</sub>)O<sub>3</sub>-Sr(Ni<sub>1/3</sub>Nb<sub>2/3</sub>)O<sub>3</sub> [10] and Ba(Zn<sub>1/3</sub>Nb<sub>2/3</sub>)O<sub>3</sub>-Sr(Zn<sub>1/3</sub>Nb<sub>2/3</sub>)O<sub>3</sub> [11], etc.

It has been found that the  $Q$  value of the dielectrics of BMT [5] and BZT [6, 7] can be improved with proper additions of Sn and Zr, respectively. In spite of the existence of Zr and Sn ions with their large ionic radii as impurities in the lattice of BZN and BMT, the spacings between ions are smaller in their respective compositions. It seems that the anharmonic interaction should decrease and thus improve the  $Q$  value [12].

Onoda *et al.* [11] suggested that an improvement in the  $\tau_f$  can be obtained by mixing different materials of  $\pm\tau_f$  such as the compound of BZN (+28 p.p.m. °C<sup>-1</sup>) and Sr(Zn<sub>1/3</sub>Nb<sub>2/3</sub>)O<sub>3</sub> (SZN, -38 p.p.m. °C<sup>-1</sup>) [11], which gives a very small  $\tau_f$  of 0.3BZN-0.7SZN to be -5 p.p.m. °C<sup>-1</sup>. Upon this consideration, BaSnO<sub>3</sub> with its negative  $\tau_f$  added to BZN forming the compound (1-x)BZN-xBaSnO<sub>3</sub> with minor  $\tau_f$  is, therefore, predictably achieved.

The main purpose of this study was to survey the microwave properties of (1-x)BZN-xBaSnO<sub>3</sub> dielectrics and try to use the classic dispersion theorem and logarithmic mixing rule to explain the behaviour of these dielectrics. Making use of BaSnO<sub>3</sub> as the substitutional additive in BZN, it was found, as expected, that smaller  $\tau_f$ , lower  $\epsilon_r$  and higher  $Q$  values of (1-x)BZN-xBaSnO<sub>3</sub> were attainable.

## 2. Experimental procedure

Samples were prepared from reagent grade BaCO<sub>3</sub>, ZnO, SnO<sub>2</sub> and Nb<sub>2</sub>O<sub>5</sub>. The purity of these raw powders was > 99.9%. The raw materials prepared for experiments were weighed to the composition of (1-x)Ba(Zn<sub>1/3</sub>Nb<sub>2/3</sub>)O<sub>3</sub>-xBaSnO<sub>3</sub> (0 ≤ x ≤ 0.32).

The starting powders were mixed in a ball mill in a plastic pot with agate balls and distilled water for 12 h, then dried and calcined at 1100 °C for 2 h. The powders were then milled again with organic binder for forming granulation. Cylindrical specimens were pressed under a pressure of 2000 Kg cm<sup>-2</sup> then debinded for 20 h at 650 °C. These pellets were sintered in air at 1380, 1430, 1470 and 1500 °C. The density of these ceramics was measured by the Archimedes method. The porosity ratio of a specimen was estimated as

$$\text{porosity (\%)} = \frac{(D_1 - D_2)}{D_1} \times 100\% \quad (1)$$

where  $D_1$  and  $D_2$  are the X-ray theoretical density and the measured density, respectively.

The post method (Fig. 1), first introduced by Hakki and Coleman [13] then modified by Courtney [14], was applied to estimate the  $\epsilon_r$  of DRs. The Kobayashi

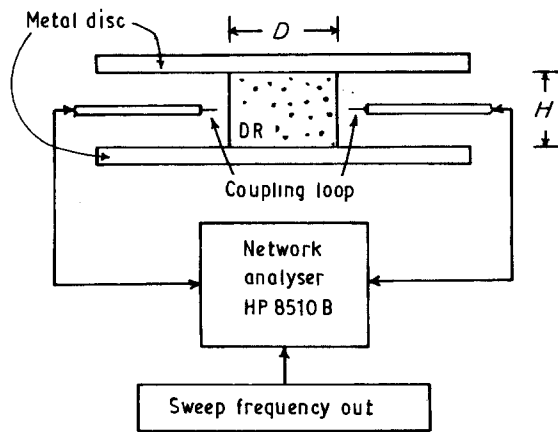


Figure 1 The post method with a radial dielectrometer for microwave dielectric measurements.

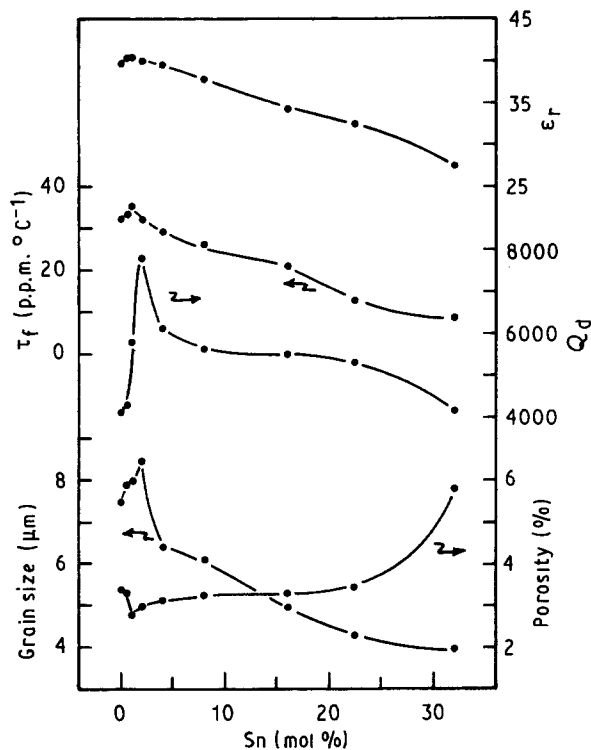


Figure 2 Microwave dielectric properties, at 10 GHz, of  $\text{Ba}(\text{Sn}_x\text{Zn}_{1-x})_{1/3}\text{Nb}_{2/3}\text{O}_3$  compositions, calcined at  $1100^\circ\text{C}$  for 2 h and sintered for 6 h at  $1430^\circ\text{C}$ , as a function of the Sn content.

and Katoh method [15] and that of Higashi and Makino [16] were utilized to measure the  $Q_d$  and  $\tau_f$  values, respectively, of DRs. Experimental equipment included the HP8350B + HP83592A sweep oscillator and the HP8510B network analyser.

X-ray diffraction (XRD) analysis with  $\text{CuK}\alpha$  radiation through a nickel filter, scanning electron microscopy (SEM) and energy-dispersive X-ray spectrometry (EDS) were utilized to investigate the microstructures of the dielectrics.

### 3. Results

Fig. 2 shows the microwave dielectric properties of  $(1-x)\text{Ba}(\text{Zn}_{1/3}\text{Nb}_{2/3})\text{O}_3-x\text{BaSnO}_3$  ( $0 \leq x \leq 0.32$ ), sintered at  $1430^\circ\text{C}$  for 6 h, as a function of the Sn content at 10 GHz. It can be seen that  $\epsilon_r$  decreased with

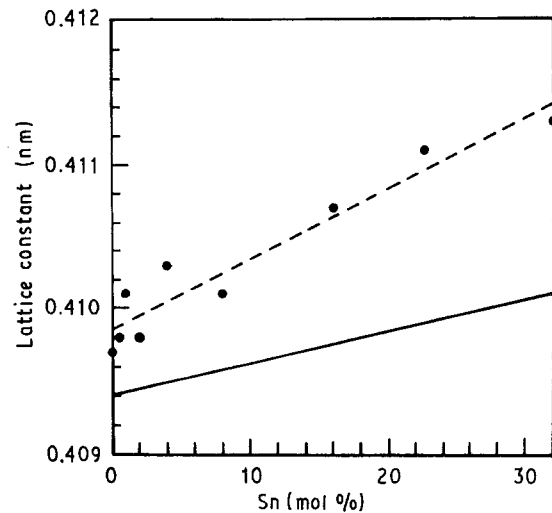


Figure 3 The lattice constant of  $(1-x)\text{BZN}-x\text{BaSnO}_3$  compositions with various Sn contents: (—) theory and (---) experiment.

increasing  $\text{BaSnO}_3$  when its content was  $> 1$  mol %. When  $\text{BaSnO}_3$  was added to 2 mol %,  $\epsilon_r \approx 40$  and  $Q_d > 7500$  were obtained; however, its  $\tau_f$  ( $> +30$  p.p.m.  $^\circ\text{C}^{-1}$ ) was too large to be used in practice. It was found that  $\tau_f$  decreased with increasing Sn content when the quantity was  $> 1$  mol %. In addition, when the Sn content was  $> 30$  mol %, a small  $\tau_f$  of  $+9$  p.p.m.  $^\circ\text{C}^{-1}$  and a small  $Q_d$  value of 4100 were obtained. For the considerations of small  $\tau_f$  and available  $Q$  value of a DR, the composition of  $0.774\text{Ba}(\text{Zn}_{1/3}\text{Nb}_{2/3})\text{O}_3-0.226\text{BaSnO}_3$  (BSZN) was chosen as the fundamental composition for further study in this work.

According to the Joint Committee on Powder Diffraction Standards international centre for diffraction data, BZN and  $\text{BaSnO}_3$  were indexed on the same perovskite cubic cell with lattice constant of  $a = 0.4094$  and  $a = 0.41163$  nm, respectively. The lattice constant of  $(1-x)\text{BZN}-x\text{BaSnO}_3$  was calculated on the assumption that it is a linear combination of BZN and  $\text{BaSnO}_3$  initially. This hypothesis (full line) was verified by the experimental XRD data (closed circles) shown in Fig. 3 with errors  $< 0.001$  nm. Therefore, the theoretical curve of lattice constant  $a$  in Fig. 3 can be thought of as almost the same as the presumptive value of a linear combination of  $(1-x)\text{BZN}$  and  $x\text{BaSnO}_3$ . The broken line in Fig. 3 is derived by curve fitting of the XRD experimental results, where

$$a = 0.048261x + 4.0987 \quad (2)$$

The grain size of  $(1-x)\text{BZN}-x\text{BaSnO}_3$  in Fig. 2 indicates that it initially increased with Sn content. When the amount of Sn was  $> 2$  mol %, grain growth was evidently inhibited with the suppression of  $\epsilon_r$ , yet the number of pores increased in the meantime. Consequently,  $\text{BaSnO}_3$  acted as a sintering promoter when the quantity of it added to BZN was  $< 2$  mol %. For the case of  $> 30$  mol % Sn added specimens with small grainsize, rich porosity as well as low  $Q_d$  value were found (Fig. 2).

The effects of sintering at various temperatures for 6 h on the microwave dielectric properties of

Ba(Sn<sub>0.226</sub>Zn<sub>0.258</sub>Nb<sub>0.516</sub>)O<sub>3</sub> (BSZN) are shown in Fig. 4. The figure indicates that the  $\tau_r$  and  $\epsilon_r$  decreased slightly with sintering temperature. However, the  $Q_d$  values of BSZN increased with sintering temperature. An obvious increase was found starting at 1430 °C, and then gradually peaked when the temperature was above 1470 °C, with  $Q_d > 9000$ . The  $Q_d$  value was determined as 9700 at 10 GHz when the BSZN composition was sintered at 1500 °C for 6 h, for which an  $\epsilon_r$  of 32 and smaller  $\tau_r$  of +12 p.p.m. °C<sup>-1</sup> were achieved. The grain size of BSZN had almost the same trend as the  $Q_d$  values, with the porosity ratio increasing slightly from 4.1 to 4.6% as shown in Fig. 4.

Fig. 5 shows the microwave dielectric properties of the BSZN dielectrics as a function of the sintering time at 1380 °C. It was found that  $\epsilon_r$  was not sensitive to the sintering conditions, whereas the value of  $Q_d$  evidently depended on it. The grain size seemed to have no obvious change with sintering time. The XRD patterns of the sintered surface of BSZN are shown in Fig. 6. The patterns in Fig. 6a–c indicate its surface unpolished, polished once (about 0.2 mm removed) and polished twice (about 0.4 mm removed), respectively. It is difficult to identify the new phases shown in Fig. 6a and b with the existing powder diffraction file.

It was found that the Sn, Zn and Nb evaporated during sintering because diminished contents of them were observed by the EDS analyses. This explains the new peaks in the XRD diffraction patterns taken from the sintered surface of BSZN in Fig. 6a and b. These new peaks disappeared in Fig. 6c, showing that the bulk of BSZN has a simple cubic perovskite unit cell. The volatile materials were found to be diminished within about 0.4 mm. The depletion of these volatile materials increased with sintering time, and its effects

on the surface of BSZN can be seen in Fig. 7a–c. Fig. 7 shows surface SEM micrographs of BSZN under various sintering conditions. The number of pores of the BSZN ceramics was found to be slightly increased with sintering time and temperature, as shown in Figs 4, 5 and 7.

#### 4. Discussion

Principally, the  $\tau_r$  and  $\epsilon_r$  of the solid solution of (1 - x) BZN-xBaSnO<sub>3</sub> can be explained by the logarithmic mixing rule with three elements which includes BZN ( $\epsilon_r = 40$ , temperature coefficient of dielectric constant  $\tau_\epsilon = -78$  p.p.m. °C<sup>-1</sup>) [8], BaSnO<sub>3</sub> ( $\epsilon_r = 14$ ,  $\tau_\epsilon = +180$  p.p.m. °C<sup>-1</sup>) and pores filled with air ( $\epsilon_r = 1$ ,  $\tau_\epsilon = 0$  p.p.m. °C<sup>-1</sup>). In essence, the temperature coefficient of resonant frequency  $\tau_r$  of a dielectric

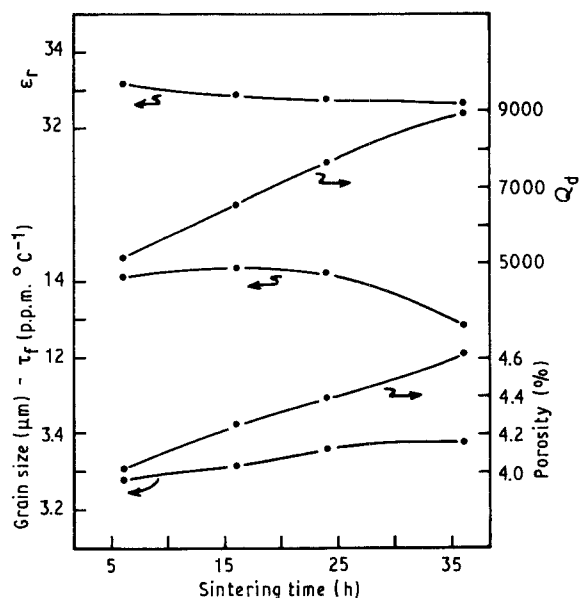


Figure 5 Microwave dielectric properties of the Ba(Sn<sub>0.226</sub>Zn<sub>0.258</sub>Nb<sub>0.516</sub>)O<sub>3</sub> (BSZN) ceramics sintered at 1380 °C as a function of the sintering time.

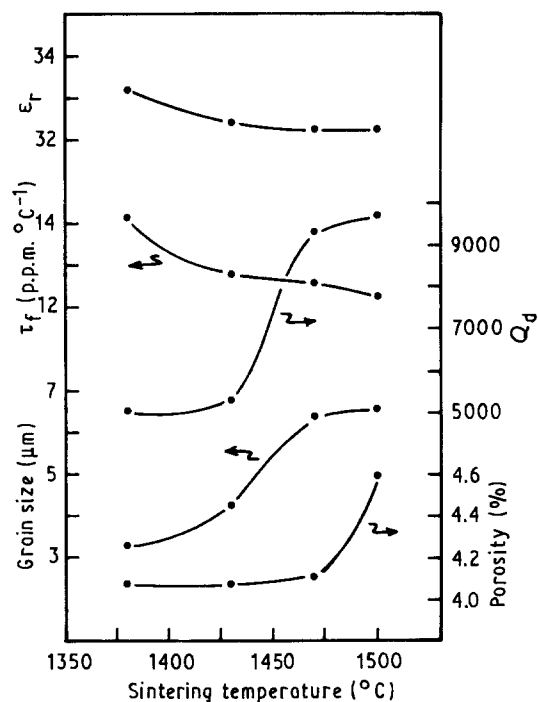


Figure 4 Microwave dielectric characteristics of Ba(Sn<sub>0.226</sub>Zn<sub>0.258</sub>Nb<sub>0.516</sub>)O<sub>3</sub> (BSZN) ceramics sintered for 6 h at various temperatures.

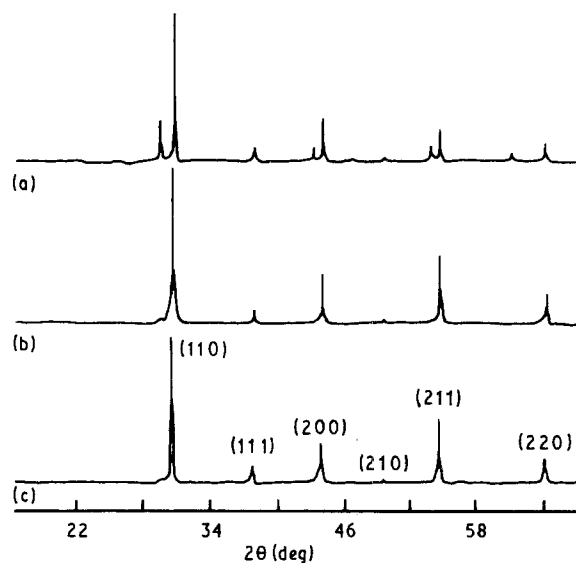


Figure 6 XRD patterns on the Ba(Sn<sub>0.226</sub>Zn<sub>0.258</sub>Nb<sub>0.516</sub>)O<sub>3</sub> (BSZN) sintered surface, where the surface is (a) unpolished; (b) polished once, about 0.2 mm removed and (c) polished twice, about 0.4 mm removed.

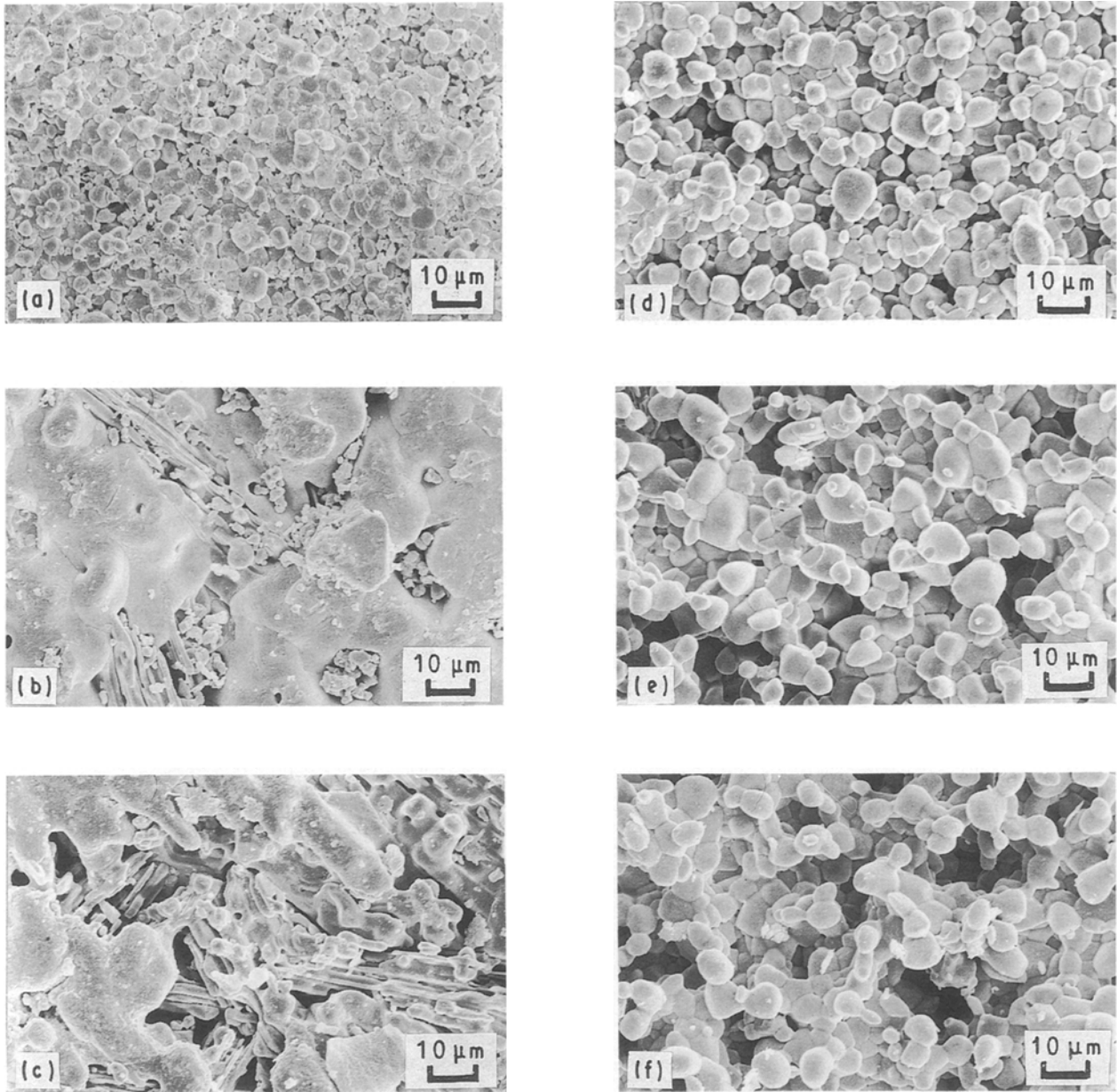


Figure 7 Surface SEM micrographs of the  $0.774\text{BZN}-0.226\text{BaSnO}_3$  dielectrics under various sintering conditions: (a)  $1380^\circ\text{C}$  for 6 h, (b)  $1380^\circ\text{C}$  for 24 h, (c)  $1380^\circ\text{C}$  for 36 h, (d)  $1430^\circ\text{C}$  for 6 h, (e)  $1470^\circ\text{C}$  for 6 h and (f)  $1500^\circ\text{C}$  for 6 h.

is a function of the thermal expansion coefficient ( $\alpha$ ) and the temperature coefficient of dielectric constant ( $\tau_\epsilon$ ), where  $\tau_f \approx -(\alpha + \frac{1}{2}\tau_\epsilon)$  [17]. It was seen that the  $\epsilon_r$  of  $(1-x)\text{BZN}-x\text{BaSnO}_3$  decreased with the  $\text{BaSnO}_3$  content when its amount was  $> 1$  mol %. The  $\epsilon_r$  of  $0.999\text{BZN}-0.01\text{BaSnO}_3$  is slightly higher than that of BZN, owing to its minor porosity content. However, with more Sn added,  $\epsilon_r$  evidently decreased owing to the increasing amount of  $\text{BaSnO}_3$  ( $\epsilon_r = 14$ ).  $\tau_f$  in Fig. 2 had a similar trend to  $\epsilon_r$ , which could also be described as due to the increase of  $\text{BaSnO}_3$  quantity which offset the  $\tau_f$  of BZN.

It is worthwhile to note that although the grainsize of  $(1-x)\text{BZN}-x\text{BaSnO}_3$  ( $0.04 \leq x \leq 0.226$ ) is smaller than that of BZN and the porosity ratio of its relative composition is not less than that of BZN, the  $Q_d$  values of  $\text{Ba}(\text{Sn}_x\text{Zn}_{(1-x)/3}\text{Nb}_{(1-x)/3})\text{O}_3$  are still higher than that of BZN (Fig. 2). Consequently, not only do the material imperfections affect the  $Q$  value of

$(1-x)\text{BZN}-x\text{BaSnO}_3$ , but some other factors also exist.

According to the classical dispersion theory [12, 18], the dielectric loss at microwave frequencies is due primarily to the damping factor of a Lorentz oscillator. The nature of this factor was ascribed to the overlapping of electron clouds of cations and anions [19]. Plendl [20] calculated this factor and determined that it depends on the anharmonicity of the bonding forces and on the ratio of the cation and anion radii of a composition. It is discernible that the dielectric loss of a composition increases with increasing damping factor caused by the difference between the cation and anion radii.

The origin of the damping constant is explained by the lattice anharmonic interaction, and lattice imperfections, e.g. impurities, dislocations and grain boundaries [21]. Table I indicates the ionic radii found in several kinds of complex perovskite structures. The  $Q$

values in Table II indicate that the compositions in each group (i.e. from *a* to *d*) of  $ABO_3$  perovskite-structure having a larger ionic radius in the A site have better  $Q$  values than those with smaller ionic radii in the A site. Concurrently, the radius ratio of  $Ba^{2+}$  to  $O^{2-}$  is larger than that of  $Sr^{2+}$  to  $O^{2-}$ , and therefore the  $Q$  value of the former is greater than that of the latter. Furthermore, the average radius of B-site ions of  $Ba(Sn,Zn,Nb)O_3$  ( $a_3$ ),  $Ba(Sn,Mg,Ta)O_3$  ( $c_2$ ) and  $Ba(Zr,Zn,Ta)O_3$  ( $d_3$ ) in Table II are also larger than those structures without Sn, Sn and Zr, respectively. This brings the B-site cations' average radius and the anion radius of oxygen closer, so the spacings between ions become smaller. This decreases the anharmonic interaction, and higher  $Q$  values are obtained.

With more than 2 mol % Sn added to BZN, a smaller grainsize and more pores (Fig. 2) of  $(1-x)BZN-xBaSnO_3$  were found; the increase in these imperfections will cause a decrease in the  $Q$  values. Consequently, due to the increase of the imperfect damping factor and anharmonic interaction, the gain in  $Q$  value by addition of Sn described above is offset. When the amount of Sn added increased to 32 mol %, the  $Q$  value apparently decreased to 4100.

Fig. 4 shows the grainsize increased with sintering temperature from 1380 to 1470 °C with a slightly

increasing porosity. This might cause a decrease in the number of imperfections and the improvement of  $Q$  values. When the sintering temperature was above 1470 °C the effects of pores in the dielectric bulk offset the  $Q$  value upgrade to a saturated level. The presence of new phases on the sintered surface of BSZN, shown in Fig. 6a and b, shown by the appearance of new XRD peaks, is due to the depletion of the volatile materials of Sn, Zn and Nb. The amount of these vanished materials estimated by EDS analyses increased with sintering temperature and sintering time. However, the real effects caused by these volatile phenomena on the microwave dielectric properties of BSZN are not very clear and warrant further study.

Surface SEM micrographs of BSZN under various sintering conditions are shown in Fig. 7. Note that if the sintering time is  $> 24$  h at 1380 °C the loss of the volatile materials Sn, Nb and Zn on the surface of BSZN causes the appearance of new phases in Fig. 7b and c. This can be verified by XRD analysis (Fig. 6a). Obviously, the grainsize of the BSZN specimen sintered at 1430 °C for 6 h shown in Fig. 7d is greater than that at 1380 °C for 6 h shown in Fig. 7a, which can be also seen in Fig. 4. In addition, the porosity ratio of BSZN at the various sintering temperatures in Fig. 7c–e is also indicated in Fig. 4.

TABLE I Table of ionic radii

Ion	Radius (nm)
$O^{2-}$	0.140
$Ba^{2+}$	0.136
$Sr^{2+}$	0.116
$Zn^{2+}$	0.075
$Mg^{2+}$	0.072
$Ni^{2+}$	0.069
$Zr^{4+}$	0.072
$Sn^{4+}$	0.069
$Ta^{5+}$	0.064
$Nb^{5+}$	0.064

## 5. Conclusions

We investigated the dielectric properties of the  $Ba(Sn_x Zn_{(1-x)/3} Nb_{(1-x)/3})O_3$  ( $0 \leq x \leq 0.32$ ) system at microwave frequencies and found that the  $Ba(Sn_{0.226} Zn_{0.258} Nb_{0.516})O_3$  (BSZN) dielectrics have excellent properties for use as microwave devices. The  $\epsilon_r$ ,  $\tau_f$  and  $Q$  value of the  $(1-x)BZN-xBaSnO_3$  compositions can be mostly explained by the logarithmic mixing rule and classical dispersion theory; respectively. With the addition of  $BaSnO_3$  to  $Ba(Zn_{1/3} Nb_{2/3})O_3$ , the average radius of the B-site ions of  $ABO_3$  increased. This reduced the ionic radius difference between the average cation radius of the B site and the anion radius of oxygen; since the Sn ion has a larger ionic radius, the spacings between ions

TABLE II The  $Q$  values of several kinds of complex perovskite dielectrics

Group	Composition	$Q$ value	Reference
$a_1$	$Sr(Zn_{1/3} Nb_{2/3})O_3$	2000 (10 GHz)	[11]
$a_2$	$Ba(Zn_{1/3} Nb_{2/3})O_3$	5400 (10 GHz)	[11]
$a_3$	$Ba(Sn_{0.226} Zn_{0.258} Nb_{0.516})O_3$	9700 (10 GHz)	Present
$b_1$	$Sr(Ni_{1/3} Nb_{2/3})O_3$	3180 (9 GHz)	[22]
$b_2$	$Ba(Ni_{1/3} Nb_{2/3})O_3$	4000 (9 GHz)	[22]
$c_1$	$Ba(Mg_{1/3} Ta_{2/3})O_3$	6000 (10 GHz)	[5]
$c_2$	$Ba(Sn_{0.14} Mg_{0.27} Nb_{0.59})O_3$	10 800 (10 GHz)	[5]
$d_1$	$Sr(Zn_{1/3} Ta_{2/3})O_3$	3100 (7 GHz)	[6]
$d_2$	$Ba(Zn_{1/3} Ta_{2/3})O_3$	9800 (7 GHz)	[6]
$d_3$	$Ba(Zr_{0.05} Zn_{0.32} Ta_{0.63})O_3$	14 800 (7 GHz)	[6]

become smaller in the Ba(Sn,Zn,Nb)O<sub>3</sub> solid solution and the anharmonic interaction is decreased.

The resultant composition of BSZN gives a high-*Q*, temperature-stable, well-sintered dielectric resonator for use at microwave frequencies. In this study the *Q*<sub>d</sub> value of BZN could be improved by the proper addition of Sn, and the resultant composition of the BSZN could be greatly improved by increasing the sintering temperature or prolonging the sintering time. Under calcination at 1100 °C for 2 h and sintering at 1500 °C for 6 h, the τ<sub>f</sub> of +12 p.p.m. °C<sup>-1</sup> and the high *Q*<sub>d</sub> value of 9700 of Ba(Sn<sub>0.226</sub>Zn<sub>0.258</sub>Nb<sub>0.516</sub>)O<sub>3</sub> dielectrics were achieved.

### Acknowledgement

The authors thank the National Science Council, Republic of China, for their financial support under grant NSC-80-0404-E006-16.

### References

1. R. D. RICHTMYER, *J. Appl. Phys.* **10** (1939) 391.
2. J. PUSATI, *Microwaves RF* **26** (1987) 76.
3. J. S. SUN, L. WU and C. C. WEI, *ibid.* **29** (1990) 93.
4. Y. KOBAYASHI and M. MINEGISHI, *IEEE Trans. Microwave Theory Technol* **35** (1987) 1156.
5. T. KONOIKE and H. TAMURA, US Patent 4 585 744 (1986).
6. H. TAMURA, T. KONOIKE, Y. SAKABE and K. WAKINO, *J. Amer. Ceram. Soc.* **67** (1984) C59.
7. K. WAKINO, D. A. SAGALA and H. TAMURA, *Jpn. J. Appl. Phys.* **24** (1985) 1042.
8. S. KAWASHIMA, M. NISHIDA, I. UEDA and K. OUCHI, in Institute of Electronics Communication Engineers of Japan MW 80-29 (1980) 1.
9. *Idem.*, *Natn. Tech. Rep.* **28** (1982) 1108.
10. H. BANNO, F. MIZUNO, T. TAKEUCHI, T. TSUNOOKA and K. OHYA, *Jpn. J. Appl. Phys.* **24** (1985) 87.
11. M. ONODA, K. KUWATA, K. KANETA, K. TOYAMA and S. NOMURA, *ibid.* **21** (1982) 1707.
12. I. BUNGET and M. POPESCU, in "Physics of Solid Dielectrics" (Elsevier Science, New York, 1984) p. 217.
13. B. W. HAKKI and P. D. COLEMAN, *IRE Trans. Microwave Theory Technol.* **16** (1960) 402.
14. W. E. COURTNEY, *IEEE Trans. Microwave Theory Technol.* **18** (1970) 476.
15. Y. KOBAYASHI and M. KATOH, *ibid.* **33** (1985) 586.
16. T. HIGASHI and T. MAKINO, *ibid.* **29** (1981) 1408.
17. D. KAJFEZ and P. GUILLON, in "Dielectric Resonators" (Artech House, Massachusetts, 1986) p. 345.
18. G. BURNS, in "Solid State Physics" (IBM, Yorktown Heights, New York, 1985) p. 461.
19. J. N. PLENDL, A. HADNI, Y. HENNENGER, F. MORLOT, P. STRIMER and L. C. MANSUR, *Appl. Opt.* **1** (1966) 397.
20. J. N. PLENDL, in "Far Infrared Properties of Solid" (Plenum Press, New York, 1970) p. 387.
21. B. D. SILVERMAN, *Phys. Rev.* **125** (1962) 1921.
22. T. KAKEHIRO and H. TAMURA, US Patent 4 585 744 (1986).

Received 23 November 1991  
and accepted 2 September 1992